Elucidation of the Effects of the Cellular Environment on the UNCG Hairpin Motif

A Senior Honors Thesis

Submitted in Partial Fulfillment of the Requirements
for Graduation in the Honors College

By

Michelle Whittum

Biochemistry Major

The College at Brockport
May 13, 2016

Thesis Director: Dr. Joshua Blose, Assistant Professor, Chemistry

Table of Contents

Acknowledgments

First and foremost, I want to thank my research advisor Dr. Joshua Blose for all of his guidance and support over the past three years. Dr. Blose, you have been a wonderful mentor and biochemistry professor.

I want to thank the Brockport Chemistry Department for giving me the opportunity to do research as an undergraduate student. The experience enriched my education and bettered me as a biochemistry student.

I want to thank my friends and family, specifically, my mother and father for all of their support over the past three years. Creating this thesis took a great deal of focus and dedication; having the support of my loved ones is what allowed me to be successful as an undergraduate student.

Abstract

The effects of osmolytes on nucleic acid chemistry are generally not as well understood as for their protein counterparts. Recent studies have shown that these effects are rather complex and show significant dependencies on the chemical and structural properties of both the nucleic acid and the cosolute. Osmolytes have the potential to affect the stability of secondary structure motifs and alter preferences for conserved stable nucleic acid sequences. The goal of this research is to contribute to the understanding of the *in vivo* function of nucleic acids by studying the effects of different classes of osmolytes on the UNCG tetraloop motif. UNCG tetraloops are the most common and stable of the RNA tetraloops and are nucleation sites for RNA folding. UNCG loops have also been found to have a thermodynamic preference for a CG closing base pair. The thermal denaturation of UNCG containing hairpins was monitored using UV-Vis spectroscopy in the presence and absence of a series of polyols and amine-based osmolytes. Generally, the osmolytes had little effect of the thermodynamic preference for a CG closing base pair, except for PEG 200, which significantly destabilized the loops with a CG closing base pair relative to those with a GC closing base pair. Moreover this significant difference appears to be specific to UNCG loops when compared to other related sequences, suggesting that PEG 200 may have preferential interactions with the UNCG sequences in the presence of a CG closing base pair.

Introduction

Nucleic Acid Helical Structures

The most common functional structures of nucleic acids fall within three general classes of helical structures: A, B, and Z as shown in Figure 1. The A and B forms are the most common forms found *in vivo*, with the A-form primarily adopted by ribonucleic acids (RNA) and the B-form is nearly exclusive to deoxyribonucleic acid (DNA). Although DNA has the potential to fold into a variety of structural motifs beyond the double helix[1], due to its double-stranded nature and sequestering by the nucleosome, the structural complexity of DNA in vivo is significantly less than that of RNA. Two RNA strands can hybridize to form a duplex, however, most functional RNA molecules are singled-stranded molecules that fold upon themselves through intramolecular interactions including hydrogen bonding, stacking, and ionic interactions with Mg^{2+}. Through these interactions, a wide variety of secondary structural motifs such as pseudoknots and G-quadruplexes as well as complex tertiary structures can form (Figure 2).[2,3] The structural diversity of RNA is enhanced by its ability to form non-Watson Crick interactions due its single-stranded nature, and the presence of the 2′-OH which provides an additional opportunities to donate or accept a hydrogen bond at each nucleotide.

Although RNA functional structure approaches the structural complexity of that of proteins, at the base of these functional structures is the stem loop motif, which is often referred to as a hairpin. The name for this motif arises from the fact that when a single strand of RNA folds back upon itself, it resembles that of a bobby pin (Figure 3). Hairpins structures give rise to functional RNA molecules; for example, 70% of the 16 S rRNA is made of up hairpins.[4,5] Within the general class of hairpins, there are three well-studied families of tetraloops[5,6] which are given

the prefix tetra due to the four nucleotides that comprise the loop region of the hairpin. Of the known tetraloops, the UUCG is both the most common and the most stable tetraloop motif, which has been possess enhanced thermodynamic stability in the presence of a CG closing basepair.[5–8] The UUCG loops enhance RNA stability both by providing thermodynamic stability as well as chemical stability via resistance to nuclease degradation as well as promoting formation of functional structure by serving as nucleation sites for RNA folding.[7,9]

Given the importance of the UUCG hairpin motif to RNA folding and function, it serves as an excellent model upon which to determine the influence of the cellular environment. The environment of a cell is much different from that of a test tube; hairpins within the cellular environment are likely affected by the macromolecules and osmolytes surrounding them. Generally, the effects of osmolytes on nucleic acid chemistry are generally not as well understood as for their protein counterparts. Osmolytes are molecules that generally accumulate in cells under conditions of stress; the types of osmolytes that accumulate depend on the stressor (change in salinity, pressure, water content, temperature and external pressures.) as well as the type of cell.[10–12] The two classes we studied were alcohol and amine based. Sarcosine and betaine were used as amine based osmolytes; sarcosine is a metabolic intermediate and betaine accumulates in the cells of plants, animals, and bacteria to promote water retention during times of dehydration.[12,13] Polyethylene glycol (PEG), glycerol, and ethylene glycol were the alcohol based osmolytes used. Glycerol is a precursor for the synthesis of triacylglycerols and phospholipids in cells.[14] PEG is a polymer of ethylene glycol that can vary in molecular weight and which allows it to be a large enough to mimic the effects of large molecules within a cell. A cellular environment has been shown to be about 40% w/v[15]; therefore each osmolyte solution we used in the study was at this maximum concentration.

In previous studies, it has been shown that the UNCG hairpin loop is stable with a CG closing base pair in a buffered solution.[6,8] In order to gain a better understanding of how the UUCG hairpin is affected by an environment that mimics that of a cell, we studied these molecules in combination with different classes of osmolytes. The two hairpin strands we chose to study are shown, and labeled as 1cg and 1gc according to their closing base pairs (Figure 4). In making these osmolyte and hairpin solution combinations, we were attempting to understand specifically how the stability of the UUCG hairpin was affected by the other molecules in solution. The stability of a hairpin can be judged by the temperature at which it denatures and determining the free energy of the folding process. The stronger the intramolecular forces of the hairpin, the higher the temperature at which it denatures and the greater the magnitude of the free energy involved in the hairpin folding. When heat is applied to these hairpins and they unfold, and the amount of light absorbed by the RNA increases due to the hyperchromic effect. That is, with the aromatic bases no longer stacked, they are free to absorb more light. UV/Vis spectroscopy can be used to capture this change in absorbance vs. temperature during thermal denaturation and this relationship is plotted as a "melt curves". These curves can then be fit to determine the enthalpy and melting temperature of the transition, and addition parameters including the and free energy of folding can subsequently be calculated.[16] By comparing the free energy of folding for hairpins with and without osmolyte we were able to gage how each individual osmolyte impacts the structural stability of the UUCG hairpin with a CG or GC closing base pair.

For most of the osmolytes tested, we found that the destabilization per molal osmolyte (kcal mol^{-1} m^{-1}) of the both the 1cg and 1 gc hairpins agree well with literature values for a hairpin with a less table UUUU loop.[17] However, we find that PEG 200 destabilizes both hairpins at least twice as much as the other osmolytes on a per molal basis. In addition this effect is double the

destabilization afforded by urea to other RNA hairpins, and greater than the destabilization observed by the most destabilizing osmolyte, proline.[17] While all the osmolytes tested destabilized the 1cg and 1gc hairpins, none but PEG 200 influenced the thermodynamic preference for a CG closing base pair. PEG 200 showed a significant preference for destabilization of the 1cg hairpin compared to the 1 gc hairpin. Thus, PEG 200 significantly destabilized the UUCG loop with a CG closing base pair relative to the loop with the GC closing base pair. Moreover this significant difference appears to be specific to UNCG loops when compared to other related hairpin sequences (unpublished data KNL), suggesting that PEG 200 may have preferential interactions with the UNCG sequences in the presence of a CG closing base pair. This to our knowledge illustrates the first example of preferential osmolyte destabilization of a motif based solely on the identity of one base pair and one that conservatively only changes whether the purine (G) or the pyrimidine (C) is in the 5′ and the 3′ position.

Materials and Methods

Hairpin Synthesis

Integrated DNA Technologies performed solid phase synthesis to synthesize the RNA sequences studied in these experiments:

5'-rGrGrArCrUrUrCrGrGrUrCrC-3' (labeled as 1cg)

5'-rGrGrArGrUrUrCrGrCrUrCrC-3' (labeled as 1gc.)

The solutions were diluted to 1 mM using 1X TE buffer for storage. The secondary structure of each of these loops as well as the tertiary structure for 1 cg are shown in Figure 4.

Osmolyte Solution Preparation

Forty percent w/v solutions of PEG 200, ethylene glycol, glycerol, sarcosine and betaine were made in 10 mM sodium phosphate pH 7 buffer. Solutions were prepared recording both masses and volumes of components so that solution molality and molarity could also be determined.

UV-Melting Experiments

Melting measurements were recorded on at 280 nm, at 1°C per minute over a temperature range of 5 - 95°C depending on the melting temperature. Samples were prepared with 6 µL of 1 µM hairpin solution and 700 µL 40% w/v osmolyte solution. The data was normalized by dividing each absorbance by the highest absorbance recorded, and then the normalized data was fit for ΔH and T_m using a nonlinear fit model[16] on the program QtiPlot (http://www.qtiplot.com/)

Free Energy Calculations: ΔH and T_m values from the melt fits were used to solve for ΔS using $\Delta S=\frac{\Delta H}{Tm}$. ΔG was then obtained solving ΔG = ΔH -TΔS for T = 37 °C.

Results and Discussion

Figure 5 shows representative osmolyte structures and their molecular weights. Each is classified as follows: alcohols by the presences of hydroxyl group and amines by the presence of amino groups. The presence of these functional groups can impact how the hairpins fold and their stabilities; their amino and hydroxyl groups could potentially form hydrogen bonds with the hairpins. Additionally, hydrophobic interactions can occur between the hairpin molecules and the osmolytes that could influence solvation of the structures. These interactions contribute to the stability of the hairpin in solution.

Each of the above osmolytes was added to our hairpins and sodium phosphate buffer, and example melting curves from these experiments are show in Figure 6. These curves show that the addition of every osmolyte tested destabilized both the 1cg and the 1gc hairpins as each curve has a lower transition state temperature, meaning less energy was required to unfold the hairpins. Upon further quantitative thermodynamic analysis of the curves, it was determined that the stabilities of the 1cg and the 1gc hairpin folding were -5.1 kcal▪mol^{-1} and -3.3 kcal mol^{-1}, respectively (Table 1, $\Delta G°_{37\ (melt)}$). Upon the addition of osmolytes, these free energies of folding increased. This increase in the free energy of folding implies that the folding of each hairpin in less favorable in the presence of small co-solutes. This destabilization is quantitated via $\Delta\Delta G°_{37(melt,\ osmolyte)}$ which is the difference between the free energies of folding $\Delta G°_{37(melt)}$ in the presence of and absence of osmolyte. This column on the table has all positive numbers, meaning that in every case, the osmolyte destabilized the hairpin by some amount. A comparison between the free energies of folding between the 1cg and 1gc in each solution condition were also calculated, these are denoted by the column by $\Delta\Delta G°_{37\ (melt\ cg\ \ gc)}$ The positive magnitude of these $\Delta\Delta G°_{37\ (melt\ cg\ \ gc)}$ indicated that in each case, the 1cg is more stable than the 1gc in every solution condition. In order to attempt to

only account for the stability of the loop, we subtracted 0.16 kcal mol^{-1} from the $\Delta\Delta G°_{(melt, osmolyte)}$ values. The 0.16 kcal mol^{-1} parameter is to account for the contribution of the difference in the stem interactions to hairpin structure, so by removing it, we can account solely for the loop.[8,18] This value was found using *mfold*[19] and given the salt dependence of the free energy for these UUCG loops is small, the value is a reasonable estimate.[8]

Finally, the last calculation performed was the $\Delta\Delta\Delta G°_{37\ (loop,\ osmolyte)}$ which was calculated by subtracting the $\Delta\Delta G°_{37\ (loop)}$ with no osmolyte from that of the $\Delta\Delta G°_{37\ (loop)}$ with osmolytes. These values represented the differences between the stabilities of the 1cg and 1gc hairpin loops in the presence of osmolytes. In the penultimate column of Table 1, all the values are negative but within error of the measurement except for that of PEG 200 with a $\Delta\Delta\Delta G°_{37}$ (loop, osmolyte) of -0.8 kcal mol^{-1}, and -0.26 kcal mol^{-1} m^{-1}. These values represent almost an 8X to 10X times larger preference for destabilizing the CG closing base pair compared to the other osmolytes tested. This led us to become interested in how various concentrations of PEG 200 affect the stability of our hairpins. Figure 7 shows a plot of the concentration of PEG 200 vs. $\Delta G°_{37\ (melt)}$. From these results we can see that there is a linear relationship for destabilization of both the 1cg and 1 gc hairpins; however, the slope of the 1 cg curve is nearly 40% greater than that of 1 gc. Thus, as more PEG 200 is added, the preference for folding a UUCG with a CG closing base pair relative to a GC closing base pair is being diminished.

Conclusion

Our results suggest that the behavior of the UNCG hairpin within a cell is different from how it behaviors in an *in vitro* setting. Within and cell-like environment, the hairpins became significantly destabilized. In particular for PEG 200, the preference for CG over GC as a closing base pair decreased by nearly 50% of the original free energy difference. This result is significant considering only one of the tested osmolytes destabilized the hairpin in this way. PEG 200, like the other osmolytes has hydrogen bonding capabilities with the hairpin. However, PEG 200 has more hydrophobic surface area than the other tested osmolytes; it is possible these interactions could account for PEG's effect on the hairpins compared to other osmolytes and are currently under investigation. We currently have ruled out changes in salt activity as this would require a change greater than 100X based on the salt dependence of the hairpins.[8] Nevertheless, our results imply that in biological systems, nucleic acid stability can be modified upon variation in cellular concentration of osmolytes, and certain cosolutes may serve a role to either enhance or prohibit the folding of specific nucleic acids. In fact, based on these results, the conservative change of a CG to a GC closing base pair may allow for the tuning of these changes.

To further study the current outcome of these experiments, we plan to run experiments with PEG molecules of higher molecular weights. This could aid in deciphering whether the hydrophobic interactions are responsible for this destabilization, and also better mimic larger macromolecules within the cell. Additionally, we hope to run circular dichroism experiments on the hairpins in osmolyte solutions. These experiments can tell us whether the hairpins are holding into the same structures with and without osmolytes present, although it has been suggested that PEG 200 does not significantly alter hairpin structures for DNA so we do not anticipate it to do so in this case.[20]

References

(1) Kaushik, M., Kaushik, S., Roy, K., Singh, A., Mahendru, S., Kumar, M., Chaudhary, S., Ahmed, S., and Kukreti, S. (2016) A bouquet of DNA structures: Emerging diversity. *Biochem. Biophys. Reports 5*, 388–395.

(2) Draper, D. E. (2013) Folding of RNA tertiary structure: Linkages between backbone phosphates, ions, and water. *Biopolymers 99*, 1105–13.

(3) Butcher, S. E., and Pyle, A. M. (2011) The molecular interactions that stabilize RNA tertiary structure: RNA motifs, patterns, and networks. *Acc. Chem. Res. 44*, 1302–11.

(4) Gutell, R. R. (1993) Collection of small subunit (16S- and 16S-like) ribosomal RNA structures. *Nucleic Acids Res. 21*, 3051–4.

(5) Woese, C. R., Winker, S., and Gutell, R. R. (1990) Architecture of ribosomal RNA: constraints on the sequence of "tetra-loops". *Proc. Natl. Acad. Sci. U. S. A. 87*, 8467–71.

(6) Proctor, D. J., Schaak, J. E., Bevilacqua, J. M., Falzone, C. J., and Bevilacqua, P. C. (2002) Isolation and Characterization of a Family of Stable RNA Tetraloops with the Motif YNMG That Participate in Tertiary Interactions †. *Biochemistry 41*, 12062–12075.

(7) Bevilacqua, P. C., and Blose, J. M. (2008) Structures, kinetics, thermodynamics, and biological functions of RNA hairpins. *Annu. Rev. Phys. Chem. 59*, 79–103.

(8) Blose, J. M., Proctor, D. J., Veeraraghavan, N., Misra, V. K., and Bevilacqua, P. C. (2009) Contribution of the closing base pair to exceptional stability in RNA tetraloops: roles for molecular mimicry and electrostatic factors. *J. Am. Chem. Soc. 131*, 8474–84.

(9) Varani, G. (1995) Exceptionally stable nucleic acid hairpins. *Annu. Rev. Biophys. Biomol.*

Struct. 24, 379–404.

(10) Yancey, P. H., Clark, M. E., Hand, S. C., Bowlus, R. D., and Somero, G. N. (1982) Living with water stress: evolution of osmolyte systems. *Science 217*, 1214–22.

(11) Yancey, P. H. (2005) Organic osmolytes as compatible, metabolic and counteracting cytoprotectants in high osmolarity and other stresses. *J. Exp. Biol. 208*, 2819–30.

(12) Burg, M. B., and Ferraris, J. D. (2008) Intracellular organic osmolytes: function and regulation. *J. Biol. Chem. 283*, 7309–13.

(13) Gropper, S. S., and Smith, J. L. (2012) Advanced Nutrition and Human Metabolism. Cengage Learning.

(14) Jin, E. S., Sherry, A. D., and Malloy, C. R. (2013) Metabolism of glycerol, glucose, and lactate in the citric acid cycle prior to incorporation into hepatic acylglycerols. *J. Biol. Chem. 288*, 14488–96.

(15) Ellis, R. J., and Minton, A. P. (2003) Cell biology: join the crowd. *Nature 425*, 27–8.

(16) Schroeder, S. J., and Turner, D. H. (2009) Optical melting measurements of nucleic acid thermodynamics. *Methods Enzymol. 468*, 371–87.

(17) Lambert, D., and Draper, D. E. (2007) Effects of osmolytes on RNA secondary and tertiary structure stabilities and RNA-Mg2+ interactions. *J. Mol. Biol. 370*, 993–1005.

(18) Blose, J. M., Lloyd, K. P., and Bevilacqua, P. C. (2009) Portability of the GN(R)A hairpin loop motif between RNA and DNA. *Biochemistry 48*, 8787–94.

(19) Zuker, M. (2003) Mfold web server for nucleic acid folding and hybridization prediction. *Nucleic Acids Res. 31*, 3406–3415.

(20) Nakano, S.-I., Wu, L., Oka, H., Karimata, H. T., Kirihata, T., Sato, Y., Fujii, S., Sakai, H., Kuwahara, M., Kuwahara, M., Sawai, H., and Sugimoto, N. (2008) Conformation and the sodium ion condensation on DNA and RNA structures in the presence of a neutral cosolute as a mimic of the intracellular media. *Mol. Biosyst. 4*, 579–88.

Figures

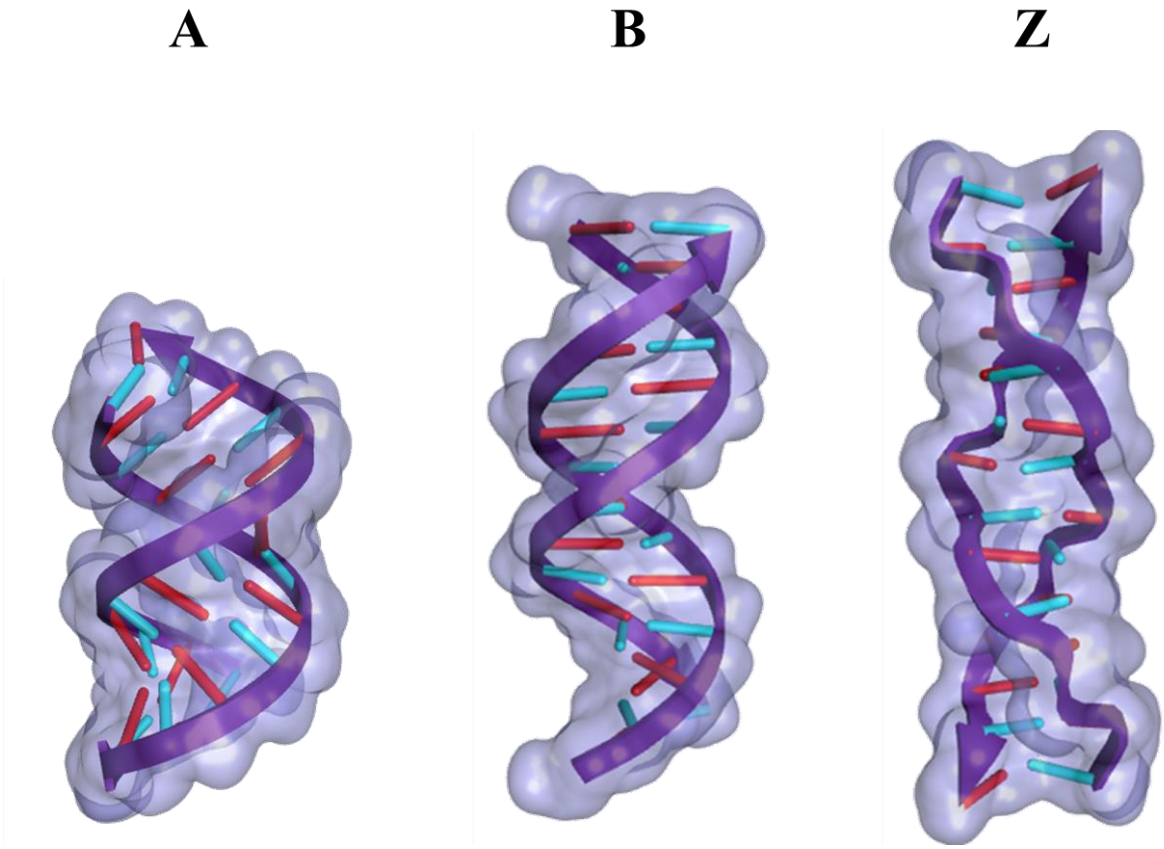

Figure 1: Nucleic Acid Helical Forms. The most common nucleic acid helical forms are shown in the figure above: A) A-Form Helix, B) B-Form Helix, and Z) Z-Form Helix. A and B form helices are both right-handed helices although B is more extended due to the absence of the 2′-hydroxyl group on the deoxyribosesugar. The Z-form helix is less common than A or B and tends to occur transiently as a part of biological processes such as transcription. The structures were generated using Discovery Studio Visualizer 4.5 (BioNova) with a solvent surface using a radius of 1.4 Å.

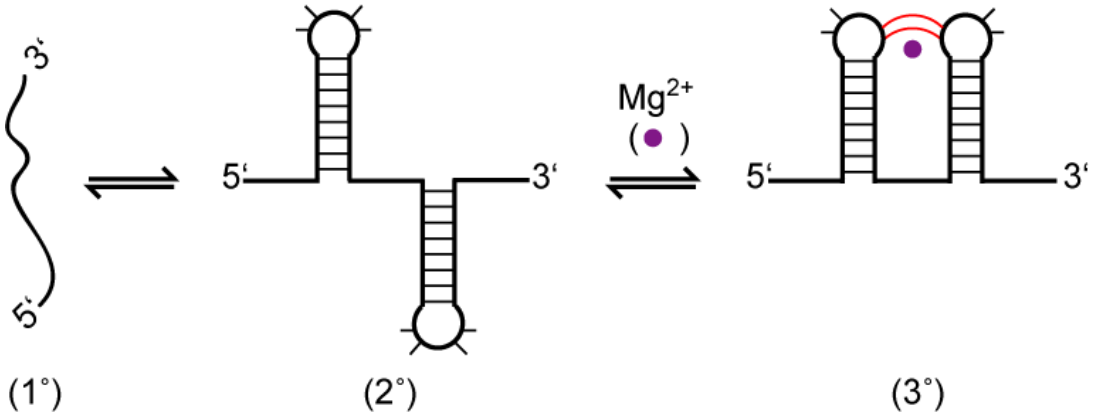

Figure 2: Folding Pathway of Single-Stranded RNA. A single-stranded RNA (1°) can fold back on itself to form base-paired regions of secondary structure (2°), that can then interact, especially in the presence of Mg^{2+} to form more complex tertiary interactions (3°)

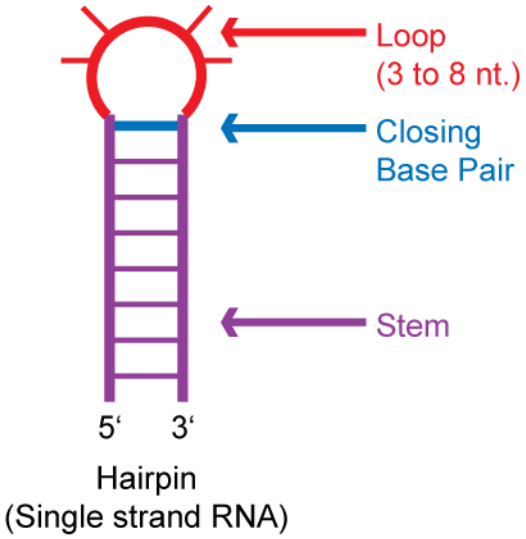

Figure 3: Structure of an RNA Hairpin. An RNA hairpin or stem-loop structure forms as the single-strand folds back on itself to form a basepaired region or stem (purple). The loop (red) typically contains 3 to 8 nucleotides that are unpaired or interact via non-Watson Crick interactions. The closing base pair (blue) is the final basepair in the stem before the loop region which has stacking interactions with the stem, but can also interact with the loop nucleotides.

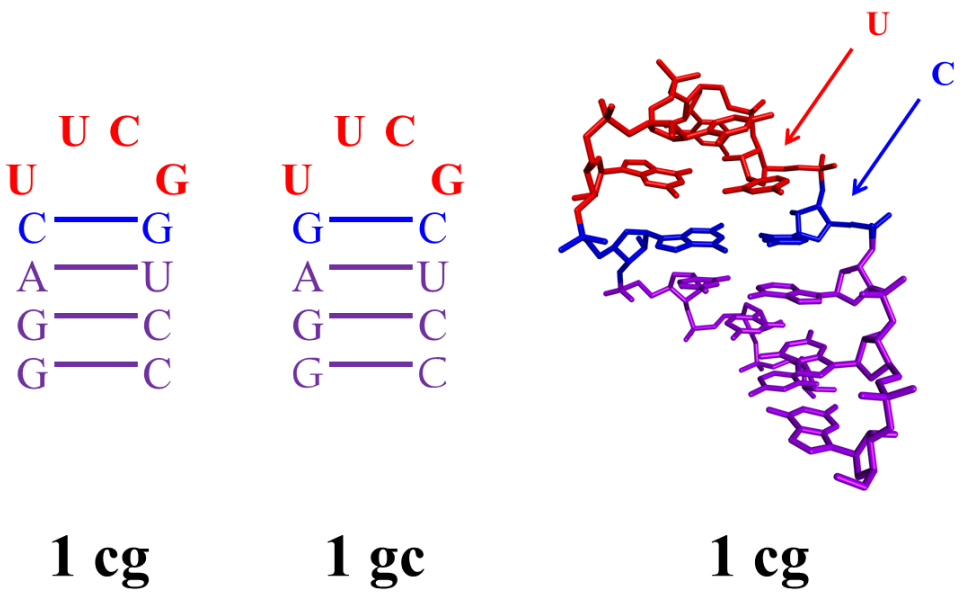

Figure 4: UNCG Tetraloop structure. The secondary structure of the 1 cg and 1 gc model hairpins used in thermal denaturation studies is shown as well as the tertiary structure for 1 cg. The stem (purple), closing basepair (blue) and loop (red) are colored for recognition in the tertiary structure of 1 cg. The C of the closing base pair and the first U of the tetraloop are highlighted. The tertiary structure is derived from PDB ID 1NBS.

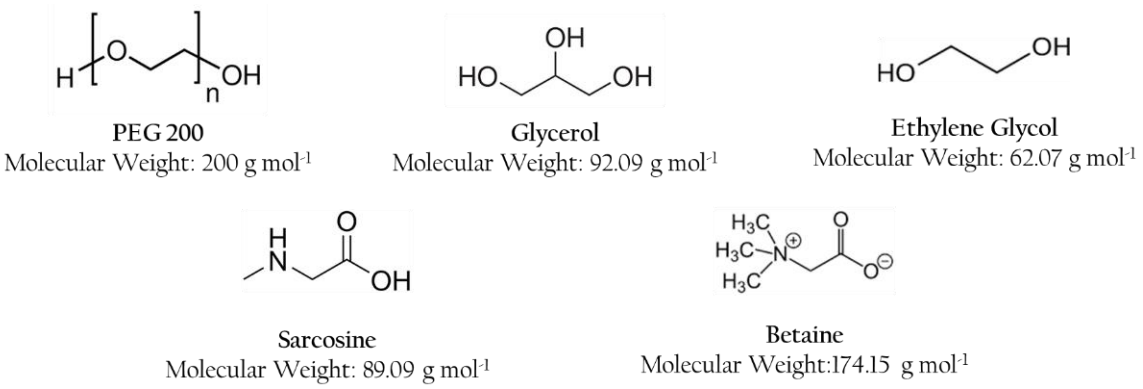

Figure 5: Example Osmolyte Structures: PEG 200 (where n=4), glycerol, ethylene glycol, sarcosine, betaine, these are grouped by the functional groups present in their structures (alcohols and amines). The molecular weights are listed below each structure.

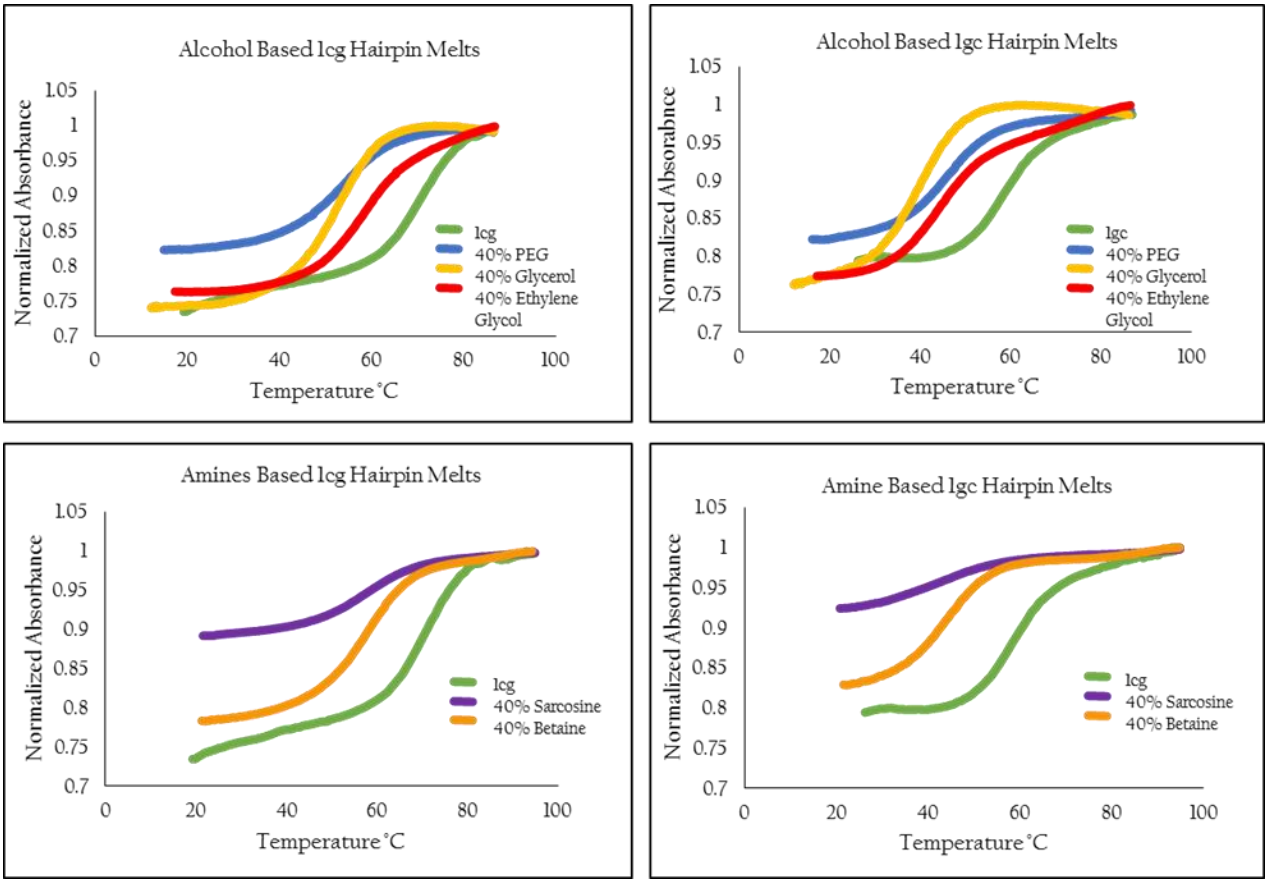

Figure 6: Example Thermal Denaturation Data. Normalized Absorbance at 280 nm is plotted vs. temperature for 1 cg and 1gc hairpins in the absence or in the presence of alcohol or amine based osmolytes. The shift of the observed transition to lower temperatures qualitatively suggests that the osmolytes are destabilizing the hairpin structures in all cases.

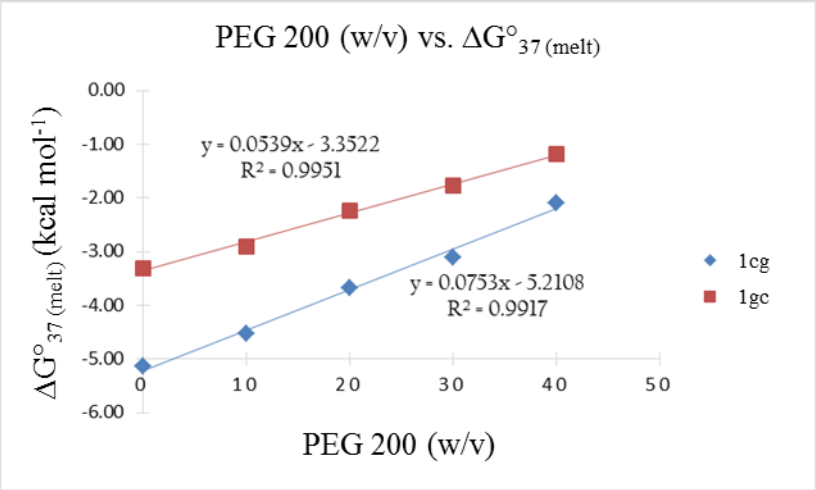

Figure 7: Relationship between PEG 200 concentration and Hairpin Stability. The $\Delta G°_{37\ (melt)}$ is plotted as a function of PEG 200 concentration (w/v) and there is a linear relationship present for both the 1cg and 1gc hairpins (R^2 = 0.9917, 0.9951, respectively), although the destabilization of 1cg is larger than that for 1gc as the slope is 40% greater for the 1cg relationship.

Table 1. Thermodynamic Parameters for Hairpin Folding

Sequence / Stem	$\Delta H°$ (kcal mol^{-1})	$\Delta S°$ (e.u.)	T_M (°C)	$\Delta G°_{37}$ (melt) (kcal mol^{-1})	$\Delta\Delta G°_{37}$ (melt, osmolyte) (kcal mol^{-1})	$\Delta\Delta G°_{37}$ (melt, osmolyte) (kcal mol^{-1} m^{-1})	$\Delta\Delta G°_{37}$ (melt cg gc) (kcal mol^{-1})	$\Delta\Delta G°_{37}$ (loop) (kcal mol^{-1})	$\Delta\Delta\Delta G°_{37}$ (loop, osmolyte) (kcal mol^{-1})	$\Delta\Delta\Delta G°_{37}$ (loop, osmolyte) (kcal mol^{-1} m^{-1})
No Osmolyte										
UUCG / 1cg	-52.3 ± 1.2	-152.2 ± 3.5	70.8 ± 0.7	-5.1 ± 0.1						
UUCG / 1gc	-48.1 ± 1.1	-144.6 ± 3.2	59.8 ± 0.6	-3.3 ± 0.1			1.8 ± 0.1	1.7 ± 0.1		
40% PEG 200										
UUCG / 1cg	-37.9 ± 1.0	-115.6 ± 2.8	55.0 ± 1.1	-2.1 ± 0.2	3.0 ± 0.1	-0.94 ± 0.03				
UUCG / 1gc	-35.9 ± 1.7	-112.3 ± 5.4	46.8 ± 0.5	-1.1 ± 0.1	2.2 ± 0.1	-0.68 ± 0.03	1.0 ± 0.1	0.8 ± 0.1	-0.8 ± 0.1	-0.26 ± 0.03
40% EG										
UUCG / 1cg	-46.3 ± 0.4	-140.8 ± 2.8	55.7 ± 0.4	-2.6 ± 0.1	2.5 ± 0.1	-0.19 ± 0.01				
UUCG / 1gc	-46.1 ± 0.6	-145.9 ± 2.2	43.2 ± 0.5	-0.9 ± 0.1	2.4 ± 0.1	-0.18 ± 0.01	1.7 ± 0.1	1.6 ± 0.1	-0.1 ± 0.1	-0.01 ± 0.01
40% Glycerol										
UUCG / 1cg	-41.1 ± 0.8	-123.9 ± 2.5	58.4 ± 0.9	-2.7 ± 0.1	2.4 ± 0.1	-0.30 ± 0.02				
UUCG / 1gc	-41.4 ± 1.0	-130.4 ± 3.1	44.2 ± 0.7	-0.9 ± 0.1	2.4 ± 0.1	-0.28 ± 0.02	1.7 ± 0.1	1.6 ± 0.1	-0.1 ± 0.1	-0.02 ± 0.02
40% Betaine										
UUCG / 1cg	-43.9 ± 1.5	-132.5 ± 4.4	58.5 ± 0.6	-2.9 ± 0.1	2.2 ± 0.1	-0.34 ± 0.02				
UUCG / 1gc	-39.7 ± 2.0	-124.8 ± 6.3	45.4 ± 0.4	-1.1 ± 0.1	2.2 ± 0.1	-0.33 ± 0.02	1.8 ± 0.1	1.6 ± 0.1	-0.0 ± 0.1	-0.01 ± 0.02
40% Sarcosine										
UUCG / 1cg	-38.1 ± 0.8	-115.1 ± 2.6	58.5 ± 0.3	-2.5 ± 0.1	2.6 ± 0.1	-0.34 ± 0.02				
UUCG / 1gc	-32.2 ± 2.1	-101.3 ± 6.5	44.8 ± 1.1	-0.8 ± 0.2	2.5 ± 0.1	-0.31 ± 0.02	1.7 ± 0.1	1.5 ± 0.1	-0.2 ± 0.1	-0.03 ± 0.02

All of these melts were performed in sodium phosphate buffer with 40% osmolyte (w/v) as described in Materials and Methods. $\Delta\Delta G°_{37(melt,\ osmolyte)}$ denotes the comparison of the free energies of folding between the same strands with and without osmolyte present; per molal (m^{-1}) values are also given. $\Delta\Delta G°_{37\ (melt\ cg\ gc)}$ denotes the change in free energy between hairpins with closing base pairs under each solution condition and $\Delta\Delta G°_{37(loop)}$ denotes this same change minus the free energy contribution of the stem. $\Delta\Delta\Delta G°_{37(loop,\ osmolyte)}$ is a comparison of the $\Delta\Delta G°_{37(loop)}$ with and without osmolytes and measures preference for the CG vs the GC closing basepair; m^{-1} values are also provided.